

On the Sensitivity of the Subspace Predictor to Behavioral Perturbations

Dian Jin, Jeremy Coulson

Abstract—Behavioral systems define discrete-time Linear Time-Invariant (LTI) systems in terms of a set of trajectories, which forms a linear subspace. This subspace underlies the subspace predictor used in data-driven prediction and control. In practice, such subspaces are typically represented through data matrices. For robustness certification and uncertainty quantification, however, these matrix representations are coordinate-dependent and therefore do not provide a coordinate-free way to quantify uncertainty. In this work, we establish two key properties of the subspace predictor. We first show that the subspace predictor is invariant under change of basis and depends only on the underlying behavioral subspace. We then derive the first explicit prediction error bound in terms of behavioral distance between the true subspace and an estimate, showing that the predictor is locally Lipschitz with respect to behavioral perturbations. We also present a one-step prediction error bound that is relevant for receding-horizon implementations which can be computed directly. Numerical experiments show that the theoretical bound upper-bounds the prediction error, and the average prediction error bound grows linearly with the behavioral distance.

Index Terms—Behavioral systems, subspace predictor

I. INTRODUCTION

Prediction from data is a canonical problem across many areas, including machine learning, signal processing, and control. A common theme across these areas is to extract low-complexity structure that can be exploited for forecasting and decision making. In systems and control, this viewpoint has given rise to subspace-based methods for system identification [1] and Data-enabled Predictive Control (DeePC) [2]. However, most existing robustness analyses are expressed in terms of matrix representations of the data [3], [4], rather than the underlying subspace itself. Consequently, they do not directly address the coordinate-free sensitivity of subspace-based prediction to perturbations. In this work, we study the robustness of subspace prediction under perturbation at the subspace level.

Behavioral systems theory [5] provides a trajectory-based viewpoint for finite-horizon LTI systems, together with a representation that can be constructed directly from data. This perspective has led to a range of data-driven simulation and control methods [2], [6]–[8]; see [9] and references therein. In particular, data-driven prediction methods utilize an offline data library collected from the system to predict the future output sequence under a prescribed future input sequence. To accommodate time-varying dynamics, recent works [10], [11] combine subspace prediction [12] with subspace tracking, modeling the evolution of system behavior

as a sequence of varying subspaces. In these approaches, the data matrix is replaced by an orthonormal basis spanning its column space. This shift from representing a behavior through a particular matrix representation to the underlying subspace naturally motivates modeling uncertainty directly at the level of subspaces. Recent works [10], [13]–[16] have adopted this geometric viewpoint, modeling uncertainty sets as collections of subspaces within a fixed distance from a nominal subspace. However, subspace discrepancy is quantified in subspace distances (e.g., chordal distance [17]), whereas prediction performance is measured in terms of output errors in the Euclidean norm. In particular, it is unclear how such geometric discrepancies affect predicted outputs. Consequently, geometric accuracy of a subspace estimate does not directly translate into performance guarantees for the resulting predictor. This work bridges this gap.

The contribution of this work is twofold. First, we quantify in Theorem 1 the sensitivity of the subspace predictor to behavioral perturbations by deriving an explicit upper bound on the prediction error in terms of the behavioral distance between the ground-truth subspace and its approximation. The bound also depends on a quantitative observability property of the system. Second, to support this perturbation analysis, we show in Theorem 2 that the subspace predictor depends only on the subspace spanned by the data matrix, rather than on the particular matrix representation itself. In other words, different data libraries spanning the same underlying subspace lead to the same prediction under the same input.

The letter is organized as follows: Section II formalizes the problem of interest. Section III contains the main results (Theorem 1 and Theorem 2). Section IV empirically studies the sensitivity of the subspace prediction in terms of the behavioral distance through a numerical case study.

Notation: The set of all nonnegative integers is denoted $\mathbb{Z}_{\geq 0}$. Given $i, j, T \in \mathbb{Z}_{\geq 0}$ with $i < j$ and a sequence $\{z(t)\}_{t=0}^{T-1} \subset \mathbb{R}^n$, define $[i, j] = [i, i+1, \dots, j-1, j]$ and $z_{[i,j]} := [z(i)^\top \ z(i+1)^\top \ \dots \ z(j)^\top]^\top$. We use $\|\cdot\|_2$ to denote both the Euclidean norm for vectors and the spectral norm for matrices, and $\|\cdot\|_F$ to denote the Frobenius norm. Given an integer $k \in \mathbb{Z}_{\geq 0}$ with $k \leq j - i + 1$, define the *Hankel matrix of depth k* associated with $z_{[i,j]}$ as

$$\mathcal{H}_k(z_{[i,j]}) := \begin{bmatrix} z(i) & z(i+1) & \dots & z(j-k+1) \\ z(i+1) & z(i+2) & \dots & z(j-k+2) \\ \vdots & \vdots & \ddots & \vdots \\ z(i+k-1) & z(i+k) & \dots & z(j) \end{bmatrix}.$$

Given $T \in \mathbb{Z}_{\geq 0}$, the sequence $z_{[0,T-1]}$ is called *persistently exciting* of order k if $\mathcal{H}_k(z_{[0,T-1]})$ has full row rank. The

Both authors are with the Department of Electrical and Computer Engineering, University of Wisconsin–Madison, Madison, WI, USA (emails: {djin38, jeremy.coulson}@wisc.edu)

Moore-Penrose inverse of a matrix M is denoted by M^\dagger . We use boldface \mathbf{U} to denote a linear subspace of \mathbb{R}^q , and plain U to denote a spanning matrix. These notations are connected by $\text{im } U = \mathbf{U}$, and will be used interchangeably. The set of orthogonal matrices is denoted $O(d) = \{U \in \mathbb{R}^{d \times d} : U^\top U = I\}$. The set of all singular values of a matrix U is denoted by $\sigma(U)$. The i^{th} singular value of a matrix U is denoted by $\sigma_i(U)$. The diagonal matrix with diagonal entries $\gamma_1, \dots, \gamma_d$ is denoted $\text{diag}(\gamma_1, \dots, \gamma_d)$. The Grassmannian is defined as $\text{Gr}(q, d) := \{\mathbf{U} \text{ is a linear subspace of } \mathbb{R}^q : \dim \mathbf{U} = d\}$. Let $\mathbf{U}, \mathbf{V} \in \text{Gr}(q, d)$ and let $U, V \in \mathbb{R}^{q \times d}$ be orthonormal bases spanning \mathbf{U} and \mathbf{V} , respectively. Consider the compact singular value decomposition (SVD) $U^\top V = P\Sigma Q^\top$, where $\Sigma = \text{diag}(\sigma_1, \dots, \sigma_d)$ with $\sigma_1 \geq \dots \geq \sigma_d \geq 0$. The principal angles $\theta_1, \dots, \theta_d \in [0, \pi/2]$ between \mathbf{U} and \mathbf{V} are given by [18] $\cos \theta_i = \sigma_i$. The *chordal distance* between \mathbf{U}, \mathbf{V} is defined equivalently by

$$d(\mathbf{U}, \mathbf{V}) = \left(\sum_{i=1}^d \sin^2 \theta_i \right)^{\frac{1}{2}} = \frac{1}{\sqrt{2}} \|UU^\top - VV^\top\|_F. \quad (1)$$

Note that the chordal distance is representation free: $d(\text{im}(UQ), \text{im}(VQ)) = d(\text{im } U, \text{im } V)$ for all $Q \in O(d)$. The Gaussian distribution with mean 0 and covariance $\Sigma \in \mathbb{R}^{d \times d}$ is denoted $\mathcal{N}(0, \Sigma)$.

II. PROBLEM STATEMENT

Consider the observable LTI dynamical system

$$\begin{aligned} x(t+1) &= Ax(t) + Bu(t), \\ y(t) &= Cx(t) + Du(t), \end{aligned} \quad (2)$$

where $A \in \mathbb{R}^{n \times n}$, $B \in \mathbb{R}^{n \times m}$, $C \in \mathbb{R}^{p \times n}$, $D \in \mathbb{R}^{p \times m}$, $x(t)$ is the state, $u(t)$ is the input, $y(t)$ is the output at time $t \in \mathbb{Z}_{\geq 0}$. The *restricted behavior* of (2) is defined as

$$\mathcal{B}_{[0, L-1]} = \left\{ (u_{[0, L-1]}, y_{[0, L-1]}) \in \mathbb{R}^{(m+p)L} \mid \text{there exists } x_{[0, L]} \in \mathbb{R}^{n(L+1)} \text{ such that (2) holds for all } t \in [0, L-1] \right\}.$$

Any $(u_{[0, L-1]}, y_{[0, L-1]}) \in \mathcal{B}_{[0, L-1]}$ is called a *trajectory* of system (2). The following lemma [9] shows that $\mathcal{B}_{[0, L-1]}$ is a linear subspace of $\mathbb{R}^{(m+p)L}$ and provides a data matrix representation.

Lemma 1 ([19, Corollary 19]). *Consider system (2). Let (A, B) be controllable and $L \geq n$. Then $\mathcal{B}_{[0, L-1]}$ is a linear subspace of dimension $\dim \mathcal{B}_{[0, L-1]} = mL + n$. Moreover, let $T \in \mathbb{Z}_{>0}$ and $(u_{[0, T-1]}, y_{[0, T-1]}) \in \mathcal{B}_{[0, L-1]}$ with $u_{[0, T-1]}$ being persistently exciting of order $n + L$, then*

$$\text{im} \begin{bmatrix} \mathcal{H}_L(u_{[0, T-1]}) \\ \mathcal{H}_L(y_{[0, T-1]}) \end{bmatrix} = \mathcal{B}_{[0, L-1]}.$$

Lemma 1 provides the foundation for viewing systems over finite horizons as subspaces [15]. The data-driven prediction problem posed in [6] aims to find the output sequence of an unknown dynamical system corresponding to an input sequence based on a past input-output trajectory collected from the system, without explicitly identifying a state-space

model. We now introduce the subspace predictor, which is the key ingredient of data-driven prediction and the main object studied in this work.

Definition 1. *Let $X \in \mathbb{R}^{(m+p)(T_{\text{ini}}+T_{\text{f}}) \times r}$, $r \in \mathbb{Z}_{>0}$. Let $(u_{\text{ini}}, u, y_{\text{ini}}) \in \mathbb{R}^{mT_{\text{ini}}+mT_{\text{f}}+pT_{\text{ini}}}$. Partition X into a block matrix*

$$X = [X_{u_p}^\top \quad X_{u_f}^\top \quad X_{y_p}^\top \quad X_{y_f}^\top]^\top,$$

where $X_{u_p} \in \mathbb{R}^{mT_{\text{ini}} \times r}$, $X_{u_f} \in \mathbb{R}^{mT_{\text{f}} \times r}$, $X_{y_p} \in \mathbb{R}^{pT_{\text{ini}} \times r}$, $X_{y_f} \in \mathbb{R}^{pT_{\text{f}} \times r}$. The subspace predictor is defined as the mapping

$$\begin{aligned} \mathcal{S} : \mathbb{R}^{(m+p)(T_{\text{ini}}+T_{\text{f}}) \times r} \times \mathbb{R}^{mT_{\text{ini}}+mT_{\text{f}}+pT_{\text{ini}}} &\rightarrow \mathbb{R}^{pT_{\text{f}}}, \\ \mathcal{S}(X, u_{\text{ini}}, u, y_{\text{ini}}) &= X_{y_f} \begin{bmatrix} X_{u_p} \\ X_{u_f} \\ X_{y_p} \end{bmatrix}^\dagger \begin{bmatrix} u_{\text{ini}} \\ u \\ y_{\text{ini}} \end{bmatrix}. \end{aligned} \quad (3)$$

Throughout this paper, the subscripts u_p, u_f, y_p, y_f always refer to this block partition for any matrices with $(m+p)(T_{\text{ini}}+T_{\text{f}})$ rows. When the vector $(u_{\text{ini}}, u, y_{\text{ini}})$ is clear from the context, we equivalently write $y_{[0, T_{\text{f}}-1]}^{\text{pred}}(X) := (y_0^{\text{pred}}(X), \dots, y_{T_{\text{f}}-1}^{\text{pred}}(X))$ for $\mathcal{S}(X, u_{\text{ini}}, u, y_{\text{ini}})$. The subspace predictor can be used to predict future output trajectories of a dynamical system given future input $u \in \mathbb{R}^{mT_{\text{f}}}$ and an initial trajectory $(u_{\text{ini}}, y_{\text{ini}}) \in \mathcal{B}_{[0, T_{\text{ini}}-1]}$ [6]. We wish to study how the perturbation to $\mathcal{B}_{[0, T_{\text{ini}}+T_{\text{f}}-1]}$ affects the subspace prediction. Let $\widehat{\mathcal{B}}_{[0, T_{\text{ini}}+T_{\text{f}}-1]}$ be the behavior of an approximate system

$$\begin{aligned} \widehat{x}(t+1) &= \widehat{A}\widehat{x}(t) + \widehat{B}u(t), \\ \widehat{y}(t) &= \widehat{C}\widehat{x}(t) + \widehat{D}u(t), \end{aligned} \quad (4)$$

where $\widehat{A} \in \mathbb{R}^{n \times n}$, $\widehat{B} \in \mathbb{R}^{n \times m}$, $\widehat{C} \in \mathbb{R}^{p \times n}$, $\widehat{D} \in \mathbb{R}^{p \times m}$. Let $u_{[0, T-1]}^{\text{d}}$ be persistently exciting of order $n + T_{\text{ini}} + T_{\text{f}}$, let $(u_{[0, T-1]}^{\text{d}}, y_{[0, T-1]}^{\text{d}}) \in \mathcal{B}_{[0, T_{\text{ini}}+T_{\text{f}}-1]}$ and $(\widehat{u}_{[0, T-1]}^{\text{d}}, \widehat{y}_{[0, T-1]}^{\text{d}}) \in \widehat{\mathcal{B}}_{[0, T_{\text{ini}}+T_{\text{f}}-1]}$. We arrange them into Hankel matrices

$$H := \begin{bmatrix} \mathcal{H}_{T_{\text{ini}}+T_{\text{f}}}(u_{[0, T-1]}^{\text{d}}) \\ \mathcal{H}_{T_{\text{ini}}+T_{\text{f}}}(y_{[0, T-1]}^{\text{d}}) \end{bmatrix}, \widehat{H} := \begin{bmatrix} \mathcal{H}_{T_{\text{ini}}+T_{\text{f}}}(\widehat{u}_{[0, T-1]}^{\text{d}}) \\ \mathcal{H}_{T_{\text{ini}}+T_{\text{f}}}(\widehat{y}_{[0, T-1]}^{\text{d}}) \end{bmatrix}. \quad (5)$$

Given $(u_{\text{ini}}, y_{\text{ini}}) \in \mathcal{B}_{[0, T_{\text{ini}}-1]}$ and an input sequence $u \in \mathbb{R}^{mT_{\text{f}}}$, we denote the predicted output sequence associated with these Hankel matrices by $y_{[0, T_{\text{f}}-1]}^{\text{pred}}(H)$ and $y_{[0, T_{\text{f}}-1]}^{\text{pred}}(\widehat{H})$. Note that $(u_{\text{ini}}, y_{\text{ini}})$ need not be a T_{ini} -length trajectory of (4), since the subspace predictor \mathcal{S} is defined for arbitrary $(u_{\text{ini}}, y_{\text{ini}}) \in \mathbb{R}^{(m+p)T_{\text{ini}}}$. This corresponds to the practical setting in which the approximate subspace, $\widehat{\mathcal{B}}_{[0, T_{\text{ini}}+T_{\text{f}}-1]}$, is used for prediction. Denote $b = (u_{\text{ini}}, u, y_{\text{ini}})$. Denote $M = [X_{u_p}^\top \quad X_{u_f}^\top \quad X_{y_p}^\top]^\top$ and similar for \widehat{M} , the prediction error can be first bounded as

$$\begin{aligned} &\|y_{[0, T_{\text{f}}-1]}^{\text{pred}}(\widehat{H}) - y_{[0, T_{\text{f}}-1]}^{\text{pred}}(H)\|_2 \\ &\leq \left(\|\widehat{H}_{y_f}\|_2 \|\widehat{M}^\dagger - M^\dagger\|_2 + \|\widehat{H}_{y_f} - H_{y_f}\|_F \|M^\dagger\|_2 \right) \|b\|_2, \\ &\leq \left(\|\widehat{H}_{y_f}\|_2 \|\widehat{M}^\dagger - M^\dagger\|_2 + \|\widehat{H} - H\|_F \|M^\dagger\|_2 \right) \|b\|_2 \end{aligned} \quad (6)$$

where the last inequality uses the fact that \widehat{H}_{y_f} and H_{y_f} are

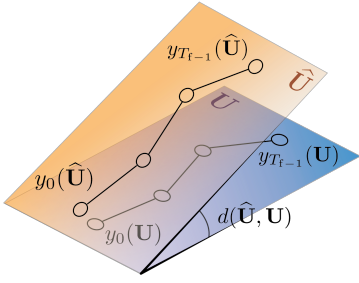


Fig. 1: The two planes represent the nominal restricted behavior \mathbf{U} and its approximation $\hat{\mathbf{U}}$, with discrepancy measured by $d(\hat{\mathbf{U}}, \mathbf{U})$.

submatrices of \hat{H} and H , respectively. However, the bound in (6) is still expressed in terms of matrix norms. As such, it is not intrinsic to the underlying restricted behaviors, and the bound may vary under different matrix representations of the same subspace. Since our goal is to relate prediction error to a geometric discrepancy between restricted behaviors, it is natural to seek a representation-free bound formulated directly in terms of $d(\text{im } \hat{H}, \text{im } H)$, see Fig. 1.

Because each restricted behavior is a linear subspace by Lemma 1, we use chordal distance d to measure discrepancy between restricted behaviors, and will refer to chordal distance and behavioral distance interchangeably. This gives rise to the central question of this letter:

Problem 1. *How do perturbations measured in chordal distance between restricted behaviors affect the subspace prediction? More precisely, how can the prediction error*

$$\left\| y_{[0, T_f-1]}^{\text{pred}}(H) - y_{[0, T_f-1]}^{\text{pred}}(\hat{H}) \right\|_2$$

be bounded in terms of $d(\text{im } H, \text{im } \hat{H})$?

We address this problem in Section III. We first examine how observability properties of (2) affect the prediction error bound given by (8), then we show that the subspace predictor \mathcal{S} is coordinate-free (Theorem 2). Finally, we relate the Frobenius norm to behavioral distance through a suitable basis representation (Lemma 3), which leads to a novel prediction error bound (Theorem 1).

III. PREDICTION ERROR BOUND

We introduce a state-space formulation of the restricted behavior. For $k \in \mathbb{Z}_{\geq 0}$, define the extended observability matrix and block Toeplitz matrix as

$$\mathcal{O}_k = \begin{bmatrix} C \\ CA \\ \vdots \\ CA^{k-1} \end{bmatrix}, \mathcal{T}_k = \begin{bmatrix} D & 0 & \dots & 0 \\ CB & D & \dots & 0 \\ \vdots & \vdots & \ddots & \vdots \\ CA^{k-2}B & CA^{k-3}B & \dots & D \end{bmatrix}.$$

Let $(u_{[0, L-1]}, y_{[0, L-1]}) \in \mathcal{B}_{[0, L-1]}$ with corresponding state sequence $x_{[0, L]}$. Denote

$$\Phi_L := \begin{bmatrix} 0 & I_{mL} \\ \mathcal{O}_L & \mathcal{T}_L \end{bmatrix},$$

then

$$\begin{bmatrix} \mathcal{H}_L(u_{[0, T-1]}) \\ \mathcal{H}_L(y_{[0, T-1]}) \end{bmatrix} = \Phi_L \begin{bmatrix} \mathcal{H}_1(x_{[0, T-L]}) \\ \mathcal{H}_L(u_{[0, T-1]}) \end{bmatrix}. \quad (7)$$

It is shown in [19, Corollary 19] that $\text{im } \Phi_L = \mathcal{B}_{[0, L-1]}$. We refer to Φ_L as the *trajectory generation matrix* of (2). The main theorem below assumes a lower bound on $\sigma_{\min}(\Phi_L)$, a quantity tied to the observability property of (2), which is analyzed in Section III-A. We now state the main theorem.

Theorem 1 (Local Lipschitz continuity of the subspace predictor). *Consider system (2). Let $T_{\text{ini}}, T_f \in \mathbb{Z}_{>0}$ and let $T_{\text{ini}} \geq n$. Let $\Phi_{T_{\text{ini}}}$ and $\Phi_{T_{\text{ini}}+T_f}$ be trajectory generation matrices of (2). Suppose there exists $\beta > 0$ such that $\sigma_{\min}(\Phi_{T_{\text{ini}}}) \geq \beta$ and let $\sigma_{\max}(\Phi_{T_{\text{ini}}+T_f}) = \alpha > 0$. Let $(u_{\text{ini}}, y_{\text{ini}}) \in \mathcal{B}_{[0, T_{\text{ini}}-1]}$, $u \in \mathbb{R}^{mT_f}$. Let H and \hat{H} satisfy $\mathcal{B}_{[0, T_{\text{ini}}+T_f-1]} = \text{im } H$ and $\hat{\mathcal{B}}_{[0, T_{\text{ini}}+T_f-1]} = \text{im } \hat{H}$. Denote $\gamma = \min(1, \beta)/\alpha$, if $d(\text{im } \hat{H}, \text{im } H) \leq \gamma/2\sqrt{2}$, then*

$$\left\| y_{[0, T_f-1]}^{\text{pred}}(\hat{H}) - y_{[0, T_f-1]}^{\text{pred}}(H) \right\|_2 \leq \left(\frac{2(1+\sqrt{5})}{\gamma^2} + \frac{1}{\gamma} \right) \sqrt{2} d(\text{im } \hat{H}, \text{im } H) \|(u_{\text{ini}}, u, y_{\text{ini}})\|_2. \quad (8)$$

Theorem 1 answers Problem 1 by quantifying how perturbations of restricted behavior, measured in behavioral distance, affect the prediction error. In particular, the bound in (8) is representation-free: it depends only on the restricted behaviors $\text{im } \hat{U}$ and $\text{im } U$, and not on the particular matrix representations. This shows that sensitivity of subspace prediction can be characterized at the geometric level. The proof of Theorem 1, presented in Section III-D, relies on three auxiliary results, developed in the following sections.

A. On the quantitative observability condition

We now turn to the assumption on $\sigma_{\min}(\Phi_{T_{\text{ini}}})$ in Theorem 1. The following proposition shows that this assumption is equivalent to observability of system (2).

Proposition 1. *Let $T_{\text{ini}} \geq n$. Then there exists $\beta > 0$ such that $\sigma_{\min}(\Phi_{T_{\text{ini}}}) \geq \beta$ if and only if $\text{rank}(\mathcal{O}_{T_{\text{ini}}}) = n$.*

Proof. Positivity of $\sigma_{\min}(\Phi_{T_{\text{ini}}})$ implies that $\Phi_{T_{\text{ini}}}$ has full column rank $n+mT_{\text{ini}}$. The upper right block $I_{mT_{\text{ini}}}$ has rank mT_{ini} , so the remaining n columns must be linearly independent, which is equivalent to $\text{rank}(\mathcal{O}_{T_{\text{ini}}}) = n$. Conversely, if $\text{rank}(\mathcal{O}_{T_{\text{ini}}}) = n$, then the structure of $\Phi_{T_{\text{ini}}}$ implies that $\Phi_{T_{\text{ini}}}$ has full column rank, and hence $\sigma_{\min}(\Phi_{T_{\text{ini}}}) > 0$. \square

This viewpoint also aligns with the quantitative observability condition [20, Eq. (20)] introduced in the robust fundamental lemma, which assumes a lower bound on $\sigma_{\min}(\Phi_{T_{\text{ini}}+T_f})$. The parameter β quantifies the *degree* of observability.

Lemma 2. *Consider system (2). Let $T_{\text{ini}} \geq n$, $T_f \in \mathbb{Z}_{>0}$. Let $V \in \mathbb{R}^{(m+p)(T_{\text{ini}}+T_f) \times r}$ be an orthonormal basis of $\text{im } \Phi_{T_{\text{ini}}+T_f}$. Denote $M = [V_{u_p}^\top \ V_{u_f}^\top \ V_{y_p}^\top]^\top$. Assume that $\sigma_{\min}(\Phi_{T_{\text{ini}}}) \geq \beta$ for some $\beta > 0$ and $\sigma_{\max}(\Phi_{T_{\text{ini}}+T_f}) = \alpha > 0$. Then M satisfies*

$$\sigma_{\min}(M) \geq \min\{1, \beta\}/\alpha.$$

The bound is also representation-free in the sense that $\sigma_{\min}(MP) \geq \min\{1, \beta\}/\alpha$ for all $P \in \mathcal{O}(r)$.

Proof. Let U be the orthonormal matrix from the QR factorization $\Phi_{T_{\text{ini}}+T_f} = UR$, where R is invertible. Then there

exists $Q \in O(r)$ such that $U = VQ$. Let Π denote the operator that selects the first $mT_{\text{ini}} + mT_{\text{f}} + pT_{\text{ini}}$ rows of a matrix such that $M = \Pi V = \Pi UQ$. Then $\Pi\Phi_{T_{\text{ini}}+T_{\text{f}}} = (\Pi VQ)R = MQR$. The matrix $\Pi\Phi_{T_{\text{ini}}+T_{\text{f}}}$ admits the form

$$\Pi\Phi_{T_{\text{ini}}+T_{\text{f}}} = \begin{bmatrix} 0 & I_{mT_{\text{ini}}} & 0 \\ 0 & 0 & I_{mT_{\text{f}}} \\ \mathcal{O}_{T_{\text{ini}}} & \mathcal{T}_{T_{\text{ini}}} & 0 \end{bmatrix} := [F \mid G]$$

where $F = \begin{bmatrix} 0 & I_{mT_{\text{ini}}} \\ 0 & 0 \\ \mathcal{O}_{T_{\text{ini}}} & \mathcal{T}_{T_{\text{ini}}} \end{bmatrix}$ and $G = \begin{bmatrix} 0 \\ I_{mT_{\text{f}}} \\ 0 \end{bmatrix}$. Since $F^\top G = 0$, the column spaces of F and G are orthogonal. Therefore for any vector $x = (x_1, x_2)$ where $x_1 \in \mathbb{R}^{mT_{\text{ini}}+pT_{\text{ini}}}$, $x_2 \in \mathbb{R}^{mT_{\text{f}}}$,

$$\begin{aligned} \|\Pi\Phi_{T_{\text{ini}}+T_{\text{f}}}x\|_2^2 &= \|Fx_1\|_2^2 + \|Gx_2\|_2^2 \\ &\geq \sigma_{\min}(F)^2\|x_1\|_2^2 + \sigma_{\min}(G)^2\|x_2\|_2^2 \\ &\geq \min(\sigma_{\min}(F)^2, \sigma_{\min}(G)^2)(\|x_1\|_2^2 + \|x_2\|_2^2) \\ &= \min(\sigma_{\min}(F)^2, \sigma_{\min}(G)^2)\|x\|_2^2. \end{aligned}$$

Now $\sigma_{\min}(G) = 1$, and $\sigma_{\min}(F) = \sigma_{\min}(\Phi_{T_{\text{ini}}}) \geq \beta$. Therefore, $\sigma_{\min}(\Pi\Phi_{T_{\text{ini}}+T_{\text{f}}}) \geq \min\{\beta, 1\}$. We have the inequality $\|XYx\|_2 \geq \sigma_{\min}(X)\|Yx\|_2 \geq \sigma_{\min}(X)\sigma_{\min}(Y)\|x\|_2$ for all $x \in \mathbb{R}^r$, where $X = \Pi\Phi_{T_{\text{ini}}+T_{\text{f}}}$, $Y = (QR)^{-1}$. Hence $\sigma_{\min}(XY) \geq \sigma_{\min}(X)\sigma_{\min}(Y)$. Since $\Phi_{T_{\text{ini}}+T_{\text{f}}}$ has full column rank and R is invertible,

$$\begin{aligned} \sigma_{\min}(M) &= \sigma_{\min}(XY) \geq \sigma_{\min}(X)\sigma_{\min}((QR)^{-1}) \\ &= \sigma_{\min}(\Pi\Phi_{T_{\text{ini}}+T_{\text{f}}})/\sigma_{\max}(QR) \\ &= \sigma_{\min}(\Pi\Phi_{T_{\text{ini}}+T_{\text{f}}})/\sigma_{\max}(R) \geq \min\{1, \beta\}/\alpha. \end{aligned}$$

Finally, since $\sigma(MP) = \sigma(M)$ for all $P \in O(r)$, we have $\sigma_{\min}(MP) = \sigma_{\min}(M)$. \square

Denote $\gamma = \min(1, \beta)/\alpha$, then we see that the bound in Theorem 1 improves as β increases, and deteriorates as α increases. In this sense, a system with stronger quantitative observability leads to a tighter bound, while a larger gain α leads to greater sensitivity to behavioral perturbations.

B. Representation-free subspace predictor

We establish that the subspace predictor depends only on the restricted behavior, rather than on the particular matrix representation.

Theorem 2. Let $T_{\text{ini}}, T_{\text{f}} \in \mathbb{Z}_{>0}$. Let $X, Y \in \mathbb{R}^{(m+p)(T_{\text{ini}}+T_{\text{f}}) \times r}$, $r \in \mathbb{Z}_{>0}$. Suppose $\text{im } X = \text{im } Y$. Assume $M = [X_{u_p}^\top X_{u_f}^\top X_{y_p}^\top]^\top$ has full column rank. Then for any $b := (u_{\text{ini}}, u, y_{\text{ini}}) \in \mathbb{R}^{m(T_{\text{ini}}+T_{\text{f}})+pT_{\text{ini}}}$,

$$\mathcal{S}(X, u_{\text{ini}}, u, y_{\text{ini}}) = \mathcal{S}(Y, u_{\text{ini}}, u, y_{\text{ini}}).$$

Proof. Since M has full column rank and M is a submatrix of X , we have $\text{rank } X = \text{rank } Y = r$. Consider the QR decompositions [18, Theorem 5.2.3] $X = UR_X, Y = VR_Y$, where $U, V \in \mathbb{R}^{(m+p)(T_{\text{ini}}+T_{\text{f}}) \times r}$ are orthonormal and $R_X, R_Y \in \mathbb{R}^{r \times r}$ are invertible. Since $\text{im } X = \text{im } Y$, we have $\text{im } U = \text{im } V$, hence $V = UQ$ for some $Q \in O(r)$. Denote $M_U = [U_{u_p}^\top U_{u_f}^\top U_{y_p}^\top]^\top$, then $M =$

$M_U R_X$, which implies M_U also has full column rank. Then $(M_U R_X)^\dagger = R_X^{-1} M_U^\dagger$. Therefore, $y_{[0, T_{\text{f}}-1]}^{\text{pred}}(X) = (U_{y_f} R_X)(M_U R_X)^\dagger b = U_{y_f} R_X (R_X^{-1} M_U^\dagger) b = U_{y_f} M_U^\dagger b$. Similarly, we have $y_{[0, T_{\text{f}}-1]}^{\text{pred}}(Y) = U_{y_f} Q R_Y (M_U Q R_Y)^\dagger b = U_{y_f} Q R_Y R_Y^{-1} (M_U Q)^\dagger b = U_{y_f} Q Q^\top M_U^\dagger b = U_{y_f} M_U^\dagger b$. Thus $y_{[0, T_{\text{f}}-1]}^{\text{pred}}(X) = y_{[0, T_{\text{f}}-1]}^{\text{pred}}(Y)$. \square

Theorem 2 implies that \mathcal{S} can be viewed as a well-defined mapping on the Grassmannian, i.e.,

$$\mathcal{S} : \text{Gr}((m+p)(T_{\text{ini}}+T_{\text{f}}), r) \times \mathbb{R}^{m(T_{\text{ini}}+T_{\text{f}})+pT_{\text{ini}}} \rightarrow \mathbb{R}^{pT_{\text{f}}},$$

$$\mathcal{S}(\mathbf{U}, u_{\text{ini}}, u, y_{\text{ini}}) = U_{y_f} \begin{bmatrix} U_{u_p} \\ U_{u_f} \\ U_{y_p} \end{bmatrix}^\dagger \begin{bmatrix} u_{\text{ini}} \\ u \\ y_{\text{ini}} \end{bmatrix},$$

where U is an orthonormal basis of \mathbf{U} . When the vector $(u_{\text{ini}}, u, y_{\text{ini}})$ is clear from context, the notations

$$\mathcal{S}(\mathbf{U}), \mathcal{S}(U), y_{[0, T_{\text{f}}-1]}^{\text{pred}}(U)$$

will be used interchangeably. Now we can replace H and \widehat{H} in (6) with their orthonormal bases U and \widehat{U} , respectively. Then (6) reveals two sources of prediction error: one through the sensitivity of M^\dagger , governed by the singular values of M , and the other is related to the matrix norm $\|\widehat{U} - U\|_F$ which depends on the basis representations of the restricted behaviors $\text{im } \widehat{H}$ and $\text{im } H$. We next study the quantitative observability of (2), which is related to the magnitude of the singular values of M .

C. Basis alignment and chordal distance

The term $\|\widehat{U} - U\|_F$ in (6) depends on the particular choice of basis of $\widehat{\mathbf{U}}$ and \mathbf{U} , whereas the prediction error $\|y_{[0, T_{\text{f}}-1]}^{\text{pred}}(\widehat{U}) - y_{[0, T_{\text{f}}-1]}^{\text{pred}}(U)\|_2$ remains invariant by Theorem 2. It is therefore natural to choose orthonormal bases that minimize $\|\widehat{U} - U\|_F$. The following lemma is classical and closely related to the orthogonal Procrustes problem [21]. We include it here for completeness, since the proof highlights the geometric role of principal angles and aligns with the subspace-based viewpoint adopted in this work.

Lemma 3. Let $\mathbf{U}, \widehat{\mathbf{U}} \in \text{Gr}((m+p)L, r)$ with orthonormal bases U and \widehat{U} , respectively. Let $\theta_1, \dots, \theta_r$ be the principal angles between \mathbf{U} and $\widehat{\mathbf{U}}$. Then

$$\min_{R \in O(r)} \|U - \widehat{U}R\|_F^2 = 2r - 2 \sum_{i=1}^r \cos \theta_i.$$

The minimum is attained at $R^* = QP^\top$, where $U^\top \widehat{U} = P \cos \Theta Q^\top$ is the compact SVD with $\cos \Theta := \text{diag}(\cos \theta_1, \dots, \cos \theta_r)$. In particular,

$$\|U - \widehat{U}R^*\|_F \leq \sqrt{2}d(\mathbf{U}, \widehat{\mathbf{U}}).$$

Proof. Let $R \in O(r)$, we have $\|U - \widehat{U}R\|_F^2 = 2r - 2\text{Tr}(U^\top \widehat{U}R)$. Denoting $S = Q^\top R P$, we have

$$\text{Tr}(U^\top \widehat{U}R) = \text{Tr}(P \cos \Theta Q^\top R) = \text{Tr}(\cos \Theta S) = \sum_{i=1}^r S_{ii} \cos \theta_i.$$

Since $S = Q^\top RP \in O(r)$, we have $|S_{ii}| \leq 1$ for $i = 1, \dots, r$. Therefore, $\text{Tr}(U^\top \widehat{U}R)$ is maximized when $R = QP^\top$, in which case $S = I_r$. Then

$$\|U - \widehat{U}QP^\top\|_F^2 = 2r - 2 \sum_{i=1}^r \cos \theta_i \leq 2 \sum_{i=1}^r \sin^2 \theta_i = 2d(\widehat{\mathbf{U}}, \mathbf{U})^2,$$

where we use the inequality $1 - \cos \theta_i \leq \sin^2 \theta_i$, which follows from $\sin^2 \theta_i - (1 - \cos \theta_i) = \cos \theta_i (1 - \cos \theta_i) \geq 0$ for all $\theta_i \in [0, \pi/2]$. \square

D. Proof of Theorem 1

By Lemma 3, once an orthonormal basis U of $\mathbf{U} = \text{im } H$ is fixed, we may choose an orthonormal basis \widehat{U} of $\widehat{\mathbf{U}} = \text{im } \widehat{H}$ so that $\|\widehat{U} - U\|_F$ is minimized. In the following, \widehat{U} denotes such a minimizing basis constructed in Lemma 3. Denote $\kappa = d(\widehat{\mathbf{U}}, \mathbf{U})$, we have $\|\widehat{U}_{y_f} - U_{y_f}\|_F \leq \|\widehat{U} - U\|_F \leq \sqrt{2}\kappa$. The difference between \widehat{M}^\dagger and M^\dagger can be bounded using results on perturbation of pseudo-inverse [22, Theorem 3.3], which implies

$$\|\widehat{M}^\dagger - M^\dagger\|_2 \leq \frac{1 + \sqrt{5}}{2} \max \left\{ \|\widehat{M}^\dagger\|_2^2, \|M^\dagger\|_2^2 \right\} \|\widehat{M} - M\|_2.$$

By Weyl's inequality [23, Eq. (3.3.19)] for singular values and Lemma 3,

$$|\sigma_{\min}(\widehat{M}) - \sigma_{\min}(M)| \leq \|\widehat{M} - M\|_2 \leq \|\widehat{M} - M\|_F \leq \sqrt{2}\kappa,$$

hence $\sigma_{\min}(\widehat{M}) \geq \sigma_{\min}(M) - \sqrt{2}\kappa \geq \gamma - \sqrt{2}\kappa$ by Lemma 2. Since $\kappa \leq \gamma/2\sqrt{2}$, then $\sigma_{\min}(\widehat{M}) \geq \gamma/2$, so $\|\widehat{M}^\dagger\|_2 = \sigma_{\min}(\widehat{M})^{-1} \leq 2/\gamma$. We then have

$$\max \left\{ \|\widehat{M}^\dagger\|_2^2, \|M^\dagger\|_2^2 \right\} \leq \max \left\{ \frac{4}{\gamma^2}, \frac{1}{\gamma^2} \right\} = \frac{4}{\gamma^2},$$

Plugging the above inequalities into (6), using Lemma 3, and using the fact that $\|\widehat{U}_{y_f}\|_2 \leq \|\widehat{U}\|_2 = 1$, we have

$$\begin{aligned} \|\mathcal{S}(\widehat{H}) - \mathcal{S}(H)\|_2 &= \|\mathcal{S}(\widehat{U}) - \mathcal{S}(U)\|_2 \\ &\leq \left(\frac{2(1 + \sqrt{5})\|\widehat{U}_{y_f}\|_2}{\gamma^2} + \frac{1}{\gamma} \right) \|\widehat{U} - U\|_F \|b\|_2 \\ &\leq \left(\frac{2(1 + \sqrt{5})}{\gamma^2} + \frac{1}{\gamma} \right) \sqrt{2}d(\widehat{\mathbf{U}}, \mathbf{U}) \|b\|_2. \end{aligned} \quad (9)$$

E. One-step prediction error bound

In many predictive control methods, only the first predicted output is used at each step. In this case, a bound on the one-step prediction error is more relevant than a bound on the full T_f -step prediction error. The remaining non-computable term is $d(\widehat{\mathbf{U}}, \mathbf{U})$, which depends on the unknown ground-truth subspace \mathbf{U} . In concrete applications such as online system identification, this quantity can be upper bounded by computable terms; see [10] for details. On the other hand, \widehat{M} is constructed from the estimated subspace and is therefore computable. This motivates a reformulation of the prediction error bound in terms of $\sigma_{\min}(\widehat{M})$, yielding a fully data-dependent and practically verifiable condition.

Corollary 1. Let $\widehat{U}_{y_f}^{(1)} := [I_p \ 0 \cdots 0] \widehat{U}_{y_f}$ which is the first p rows of \widehat{U}_{y_f} . Under the assumption of Theorem 1, except that the condition $\kappa \leq \gamma/(2\sqrt{2})$ is replaced by $\kappa \leq \sigma_{\min}(\widehat{M})/(2\sqrt{2})$, and assuming $\sigma_{\min}(\widehat{M}) > 0$, we have

$$\begin{aligned} &\|y_0^{\text{pred}}(\widehat{U}) - y_0^{\text{pred}}(U)\|_2 \leq \\ &\left(\frac{2(1 + \sqrt{5})\|\widehat{U}_{y_f}^{(1)}\|_2}{\sigma_{\min}(\widehat{M})^2} + \frac{1}{\sigma_{\min}(\widehat{M})} \right) \sqrt{2}d(\widehat{\mathbf{U}}, \mathbf{U}) \|b\|_2. \end{aligned} \quad (10)$$

Proof. Similar to (6), we also have

$$\begin{aligned} &\|y_0^{\text{pred}}(\widehat{U}) - y_0^{\text{pred}}(U)\|_2 \leq \\ &\left(\|H_{y_f}\|_2 \|M - \widehat{M}^\dagger\|_2 + \|\widehat{H}_{y_f} - H_{y_f}\|_F \|\widehat{M}^\dagger\|_2 \right) \|b\|_2. \end{aligned}$$

By Weyl's inequality used in Section III-D, we have

$$\sigma_{\min}(M) \geq \sigma_{\min}(\widehat{M}) - \sqrt{2}\kappa \geq \sigma_{\min}(\widehat{M})/2,$$

so that $\|M^\dagger\|_2 = \sigma_{\min}(M)^{-1} \leq 2/\sigma_{\min}(\widehat{M})$. Therefore, $\max\{\|M^\dagger\|_2^2, \|\widehat{M}^\dagger\|_2^2\} \leq 4/\sigma_{\min}(\widehat{M})^2$. The rest of the proof proceeds similarly as in Section III-D, which yields the bound (10). \square

IV. NUMERICAL EXPERIMENT

We illustrate the theoretical results on a LTI system¹. The goal is to explore the relationship between behavioral perturbations and the prediction error bound. Consider system (2) with $A = \begin{bmatrix} 0.8 & 0.2 \\ 0.1 & 0.9 \end{bmatrix}$, $B = [0.3 \ 0.7]^\top$, $C = [1 \ 1]$, $D = 0$. The initial state is set to $x_0 = 0 \in \mathbb{R}^2$. The true subspace \mathbf{U} is constructed via offline Hankel data collection: Let $(u_{[0, T-1]}^d, y_{[0, T-1]}^d + \eta_{[0, T-1]}^d)$ be an offline trajectory of system (2), where $\eta_t^d \in \mathcal{N}(0, \sigma \|y_t^d\|_2^2 I_p)$ with $\sigma = 0.02$ being the noise-to-signal ratio, where $u_{[0, T-1]}^d$ is persistently exciting of order $n + T_{\text{ini}} + T_f$. We vary (T_{ini}, T_f) over $\{(4, 4), (4, 2), (2, 4)\}$ and set $T = 30$. We organize the offline data into a L -depth Hankel matrix H defined by (5), where $L = T_{\text{ini}} + T_f$. We obtain an orthonormal basis $U \in \mathbb{R}^{(m+p)L \times r}$ of the subspace $\text{im } H$ through SVD. In this experiment we choose $r = mL + n$, which is the dimension of the restricted behavior of (2) by Lemma 1. We generate a family of perturbed subspaces $\{\widehat{\mathbf{U}}_n\}_{n=1}^N$ with $N = 100$. We fix an input sequence $u_{[0, T_{\text{sim}}-1]}$, and let $y_{[0, T_{\text{sim}}-1]} + \eta_{[0, T_{\text{sim}}-1]}$ to be the measured output from system (2), where $T_{\text{sim}} = 50$, $y_{[0, T_{\text{sim}}-1]}$ is the noise-free output sequence and $\eta_t \in \mathcal{N}(0, \sigma \|y_t\|_2^2 I_p)$. For each fixed $\widehat{\mathbf{U}}_n$, the T_f -length prediction at $t \in [T_{\text{ini}}, T_{\text{end}}]$ (denote $T_{\text{end}} := T_{\text{sim}} - T_f + 1$) is given by

$$\mathcal{S}(\widehat{\mathbf{U}}_n, u_{[t-T_{\text{ini}}, t-1]}, y_{[t-T_{\text{ini}}, t-1]} + \eta_{[t-T_{\text{ini}}, t-1]}),$$

and we only keep the first component, denoted by $y_t^{\text{pred}}(\widehat{\mathbf{U}}_n)$. For each $\widehat{\mathbf{U}}_n$, this yields a sequence of one-step predictions $y_{[T_{\text{ini}}, T_{\text{end}}]}^{\text{pred}}(\widehat{\mathbf{U}}_n)$. We compare these with the baseline predic-

¹The code is available at github.com/DianJin-Frederick/subspace_prediction_under_behavioral_perturbation

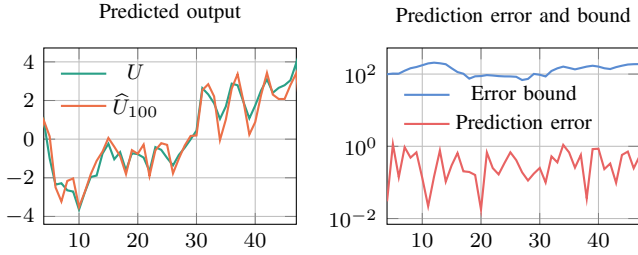


Fig. 2: Single experiment for $T_{\text{ini}} = 4$, $T_f = 2$. The left panel shows the predicted outputs generated by U and \hat{U}_{100} with $\kappa_{100} = 0.8680$. The right panel compares the corresponding prediction error and the theoretical bound (10). The horizontal axis shows the time indices $[T_{\text{ini}}, T_{\text{end}}]$.

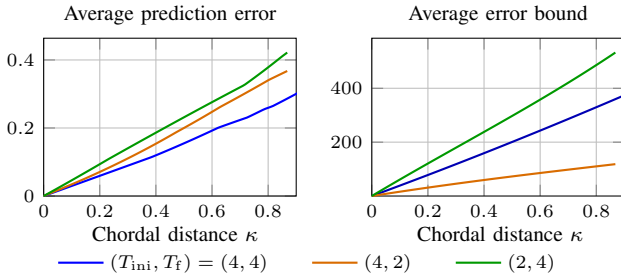


Fig. 3: Average prediction error and average prediction error bound (vertical axis) as functions of the chordal distance for three (T_{ini}, T_f) .

tions $y_{[T_{\text{ini}}, T_{\text{end}}]}^{\text{pred}}(U)$ and compute the prediction error

$$e_t^{(n)} = \|y_t^{\text{pred}}(\hat{U}_n) - y_t^{\text{pred}}(U)\|_2, \quad t \in [T_{\text{ini}}, T_{\text{end}}],$$

and the bound given by (10). We compute the average prediction error and bound over $[T_{\text{ini}}, T_{\text{end}}]$. These quantities are plotted against the chordal distance $\kappa_n = d(\hat{U}_n, U)$. Fig. 2 illustrates an experiment for \hat{U}_{100} with $\kappa_{100} = 0.8680$. The theoretical error bound correctly upper-bounds the prediction error at all t . Fig. 3 summarizes the dependence of prediction errors and bounds on the chordal distance. In all choices of (T_{ini}, T_f) , the average prediction error and bound grow approximately linearly with κ . We observe that a smaller T_f leads to a less demanding prediction task and hence a smaller prediction error. In contrast, a smaller T_{ini} provides less past information, which leads to larger prediction errors and larger bounds. This is in line with the dependence of the bound on the degree of observability, β . Despite being conservative, we empirically observe that the bound captures the linear growth rate of the prediction error in terms of the behavioral distance.

V. CONCLUSION

This work shows two fundamental properties of the subspace predictor. First, we showed that it is representation-free, in the sense that it depends only on the restricted behavior of a system. Second, we derived an explicit prediction error bound directly in terms of the chordal distance between two restricted behaviors. This provides a quantitative link between geometric uncertainty and prediction accuracy. Future work includes combining the results with computable subspace-tracking bounds, and extending the analysis from prediction to closed-loop data-driven control. We hope that the representation-free viewpoint developed will serve as a useful building block for more data-driven control methods.

ACKNOWLEDGEMENT

The authors used ChatGPT to assist with language refinement and editing in parts of this manuscript. All generated content was subsequently reviewed and edited by the authors, who take full responsibility for the final manuscript.

REFERENCES

- [1] P. Van Overschee and B. De Moor, *Subspace identification for linear systems: Theory—Implementation—Applications*. Springer Science & Business Media, 2012.
- [2] J. Coulson, J. Lygeros, and F. Dörfler, “Data-enabled predictive control: In the shallows of the DeePC,” in *2019 18th European control conference (ECC)*. IEEE, 2019, pp. 307–312.
- [3] J. Berberich, J. Köhler, M. A. Müller, and F. Allgöwer, “Data-driven model predictive control with stability and robustness guarantees,” *IEEE transactions on automatic control*, vol. 66, no. 4, pp. 1702–1717, 2020.
- [4] C. De Persis and P. Tesi, “Formulas for data-driven control: Stabilization, optimality, and robustness,” *IEEE Transactions on Automatic Control*, vol. 65, no. 3, pp. 909–924, 2019.
- [5] J. C. Willems, “From time series to linear system—Part I. Finite dimensional linear time invariant systems,” *Automatica*, vol. 22, no. 5, pp. 561–580, 1986.
- [6] I. Markovsky and P. Rapisarda, “Data-driven simulation and control,” *International Journal of Control*, vol. 81, no. 12, pp. 1946–1959, 2008.
- [7] J. Coulson, J. Lygeros, and F. Dörfler, “Distributionally robust chance constrained data-enabled predictive control,” *IEEE Transactions on Automatic Control*, vol. 67, no. 7, pp. 3289–3304, 2021.
- [8] F. Dörfler, J. Coulson, and I. Markovsky, “Bridging direct and indirect data-driven control formulations via regularizations and relaxations,” *IEEE Transactions on Automatic Control*, vol. 68, no. 2, pp. 883–897, 2022.
- [9] I. Markovsky and F. Dörfler, “Behavioral systems theory in data-driven analysis, signal processing, and control,” *Annual Reviews in Control*, vol. 52, pp. 42–64, 2021.
- [10] A. Sasfi, A. Padoan, I. Markovsky, and F. Dörfler, “Great: Grassmannian recursive algorithm for tracking & online system identification,” *IEEE Transactions on Automatic Control*, p. 11267272, 2026.
- [11] D. Jin and J. Coulson, “Online subspace learning on flag manifolds for system identification,” *arXiv preprint arXiv:2511.06416*, 2025.
- [12] W. Favoreel, B. De Moor, and M. Gevers, “SPC: Subspace predictive control,” *IFAC Proceedings Volumes*, vol. 32, no. 2, pp. 4004–4009, 1999.
- [13] A. Fazzi and I. Markovsky, “Distance problems in the behavioral setting,” *European Journal of Control*, vol. 74, p. 100832, 2023.
- [14] A. Padoan, J. Coulson, H. J. van Waarde, J. Lygeros, and F. Dörfler, “Behavioral uncertainty quantification for data-driven control,” in *2022 IEEE 61st Conference on Decision and Control (CDC)*, 2022, pp. 4726–4731.
- [15] A. Padoan and J. Coulson, “Distances between finite-horizon linear behaviors,” *IEEE Control Systems Letters*, 2025.
- [16] S. Bharadwaj, B. Mishra, C. Mostajeran, A. Padoan, J. Coulson, and R. N. Banavar, “Robust least-squares optimization for data-driven predictive control: A geometric approach,” *arXiv preprint arXiv:2511.09242*, 2025.
- [17] K. Ye and L.-H. Lim, “Schubert varieties and distances between subspaces of different dimensions,” *SIAM Journal on Matrix Analysis and Applications*, vol. 37, no. 3, pp. 1176–1197, 2016.
- [18] G. H. Golub and C. F. Van Loan, *Matrix computations*. JHU press, 2013.
- [19] I. Markovsky and F. Dörfler, “Identifiability in the behavioral setting,” *IEEE Transactions on Automatic Control*, vol. 68, no. 3, pp. 1667–1677, 2022.
- [20] J. Coulson, H. J. Van Waarde, J. Lygeros, and F. Dörfler, “A quantitative notion of persistency of excitation and the robust fundamental lemma,” *IEEE Control Systems Letters*, vol. 7, pp. 1243–1248, 2022.
- [21] P. H. Schönemann, “A generalized solution of the orthogonal procrustes problem,” *Psychometrika*, vol. 31, no. 1, pp. 1–10, 1966.
- [22] G. W. Stewart, “On the perturbation of pseudo-inverses, projections and linear least squares problems,” *SIAM review*, vol. 19, no. 4, pp. 634–662, 1977.
- [23] H. Roger and R. J. Charles, “Topics in matrix analysis,” 1994.